Virology 536 (2019) 20–26

Contents lists available at ScienceDirect

Virology

journal homepage: www.elsevier.com/locate/virology

Isoform specific editing of the coxsackievirus and adenovirus receptor

James M. Readler[a,b], Amal S. AlKahlout[c], Priyanka Sharma[c], Katherine J.D.A. Excoffon[a,b,c,*]

[a] Biomedical Sciences PhD Program, Wright State University, Dayton, OH, 45435, USA
[b] Boonshoft School of Medicine, Wright State University, Dayton, OH, 45435, USA
[c] Department of Biological Sciences, Wright State University, Dayton, OH, 45435, USA

ARTICLE INFO

Keywords:
Adenovirus
Coxsackievirus and adenovirus receptor (CAR)
Polarized epithelia
Apical and basolateral
CRISPR/Cas9 and single guide RNA (sgRNA)

ABSTRACT

The Coxsackievirus and adenovirus receptor (CAR) is both a viral receptor and cell adhesion protein. CAR has two transmembrane isoforms that localize distinctly in polarized epithelial cells. Whereas the seven exon-encoded isoform (CAR^{Ex7}) exhibits basolateral localization, the eight exon-encoded isoform (CAR^{Ex8}) can localize to the apical epithelial surface where it can mediate luminal adenovirus infection. To further understand the distinct biological functions of these two isoforms, CRISPR/Cas9 genomic editing was used to specifically delete the eighth exon of the *CXADR* gene in a Madine Darby Canine Kidney (MDCK) cell line with a stably integrated lentiviral doxycycline-inducible CAR^{Ex8} cDNA. The gene-edited clone demonstrated a significant reduction in adenovirus susceptibility when both partially and fully polarized, and doxycycline-induction of CAR^{Ex8} restored sensitivity to adenovirus. These data reinforce the importance of CAR^{Ex8} in apical adenovirus infection and provide a new model cell line to probe isoform specific biological functions of CAR.

1. Introduction

Human adenoviruses (AdV) are non-enveloped, dsDNA viruses in the *Adenoviradae* family (Berk, 2007). AdV cause a variety of diseases in humans including upper respiratory tract infections, gastroenteritis, and keratoconjunctivis (Khanal et al., 2018; Lion, 2014). While AdV infections are normally considered mild and self-limiting, severe disease sequelae, such as fulminant pneumonia, occur in immunosuppressed hosts (Echavarria, 2008; Florescu and Hoffman, 2013; Humar et al., 2005; Ison, 2006; Lion, 2014). For example, in the hematopoietic stem cell transplant setting, AdV infection prevalence ranges from 5 to 47% and mortality rates resulting from AdV infection have been reported to be as high as 80% (Echavarria, 2008).

In order to establish a respiratory infection, AdV must first gain entry to its primary target cells: the human airway epithelia of the respiratory tract. The primary receptor for all human AdV, except for group B, is the Coxsackievirus and adenovirus receptor (CAR) (Bergelson et al., 1997; Bewley et al., 1999; Walters et al., 2002). CAR is a cellular adhesion protein in the immunoglobulin superfamily that undergoes homophilic or heterophilic cell-cell adhesion with other CAR molecules on adjacent epithelial cells or junction adhesion molecule-like (JAML) expressed on the surface of leukocytes (Excoffon et al., 2005, 2007; Zen et al., 2005). The CAR-JAML interaction aids in both leukocyte transepithelial migration and adhesion at the apical surface of polarized epithelia (Kotha et al., 2015; Zen et al., 2005).

There are two transmembrane isoforms of CAR in airway epithelial cells: one encoded by the first seven exons of the *CXADR* gene (CAR^{Ex7}) and an alternatively spliced eight-exon encoded isoform (CAR^{Ex8}) (Excoffon et al., 2010, 2014). A cryptic splice site within the 7th exon allows for alternative splicing to the 8th exon resulting in distinct C-terminal sequences. These distinct C-termini result in differential localization in polarized cells (Excoffon et al., 2010, 2014; Kolawole et al., 2012; Sharma et al., 2017; Yan et al., 2015). CAR^{Ex7} localizes largely below the tight junctions where it is inaccessible to luminal AdV. CAR^{Ex8}, however, is able to localize to the apical epithelial surface where its expression correlates directly with apical AdV infection (Excoffon et al., 2010; Kotha et al., 2015). While some of the biological functions of CAR have been discovered and characterized thanks to the development of CAR knockout (KO) mice, parsing out functional differences between the CAR^{Ex7} and CAR^{Ex8} isoforms remains a challenge (Chen et al., 2006).

Our group has previously created Madin Darby Canine Kidney (MDCK) cell lines that stably express the cDNA for human CAR^{Ex8} under a doxycycline-inducible promoter in order to demonstrate the importance of increased apical CAR^{Ex8} protein expression for adenovirus infection and neutrophil adhesion (Kotha et al., 2015). To understand the effect of isoform-specific knockdown and further investigate the importance of apical CAR^{Ex8} in apical adenovirus entry and infection,

* Corresponding author. Department of Biological Sciences, Wright State University, 3640 Colonel Glenn Hwy, Dayton, OH, 45435, USA.
E-mail address: katherine.excoffon@wright.edu (K.J.D.A. Excoffon).

https://doi.org/10.1016/j.virol.2019.07.018
Received 18 March 2019; Received in revised form 22 July 2019; Accepted 23 July 2019
Available online 27 July 2019
0042-6822/

CRISPR/Cas9 technology was used, for the first time, to specifically delete the eighth exon of endogenous *CXADR*. The creation of an isoform specific knockdown cell line will allow the dissection of the biological importance of CAR^{Ex8} in viral entry and effects on leuckocyte-epithelial biology.

2. Materials and methods

2.1. Cell culture

The CAR^{Ex8} inducible MDCK cell line (MDCK-CAR^{Ex8}) was developed using the Lenti-X-Tet-On system (Takara Bio USA) on MDCK II cells (ATCC) and contains the cDNA for FLAG-tagged CAR^{Ex8} (Kotha et al., 2015). Cells are maintained in MEM media containing 5% fetal bovine serum (FBS) without tetracycline and 1% penicillin/streptomycin, at 37°C in a humidified incubator with 5% CO_2.

2.2. sgRNA development

sgRNA sequences were designed using the CHOPCHOP v2 software in conjunction with sequencing data obtained from Genewiz (South Plainfield, NJ) for the exon 8 region of the MDCK *CXADR* gene (Labun et al., 2016; Montague et al., 2014). One sgRNA upstream of exon 8 (CGAAGGGCAAAATCTTCTAG) and one sgRNA downstream of exon 8 (GGTTGCCTTGGGGAAAGTTA) were selected for subsequent experiments (IDT, Coralville, Iowa). These sgRNAs were unique in the *canis lupus familiaris* genome, with possible off target cutting sites being at least 3 nucleotides different.

2.3. Cloning

sgRNA sequences were cloned into the pspCas9(BB)-2A-GFP plasmid backbone (Addgene) using a Takara Infusion Cloning Kit (Mountain View, CA) according to the manufacturer's instructions (Ran et al., 2013). Briefly, mutagenic primers containing the sgRNA sequence to be incorporated flanked by sequence homologous to the plasmid were suggested using the Takara Primer Design tool. These primers were used in an inverse PCR reaction using CloneAmp HiFi PCR Premix (Takara Bio USA, Mountain View, CA) to linearize and incorporate each sgRNA sequence into the pspCas9(BB)-2A-GFP plasmid. For the upstream sgRNA, primer sequences were: F-GAAGGGCAAAAT CTTCTAGGTTTTAGA GCTAGAAATAGCAAGTT and R- AAGATTTTGC CCTTCGCGGTGTTTCGTCCT TTCCACAA. For the downstream sgRNA, primer sequences were: F- GTTGCCTTGGGGAAAGTTAGTTTTAGAGCT AGAAATAGCAAGTT and R- TTTCCCCAAGGCAACCCGGTGTTTCGTCC TTTCCACAA. Each linearized plasmid was then purified by treating with Cloning Enhancer and then re-circularized in an In-Fusion cloning reaction. Proper integration of each sgRNA was ensured by Sanger sequencing (Genewiz, South Plainfield, NJ) using a universal U6 primer.

2.4. Transfection

MDCK-CAR^{Ex8} cells were grown to ~60% confluence in 24-well plates. Cells were double transfected with 0.25 μg of plasmid containing the upstream and 0.25 μg of plasmid containing the downstream sgRNA using Dreamfect Gold (OZ Biosciences, San Diego, CA) transfection reagent. Cells were transfected in 100 μL of Opti-MEM at a ratio of 0.5 μg of DNA to 1 μL of transfection reagent. Cells were placed in complete media after 4 h. Optimal transfection efficiency, as measured by number of cells exhibiting GFP positivity, was reached ~48 h after transfection.

2.5. Fluorescence Activated Cell Sorting (FACS)

Two days after transfection, MDCK-CAR^{Ex8} cells were lifted using TrypLE Express (ThermoFisher Scientific, Waltham, MA) and placed in filter sterilized FACS buffer 1 mM EDTA, 25 mM HEPES, 1% FBS in phosphate buffered saline without calcium or magnesium (PBS−/−). Cells were sorted at The Ohio State University Analytical Cytometry Core. Single GFP positive cells were seeded into single wells of a 96-well plate containing normal growth media using a Becton Dickinson FACSAria III system (Franklin Lakes, NJ). Cells were maintained, changing growth media every 3–4 days until colonies could be expanded from individual cells.

2.6. PCR screening

As colonies grew to confluence, they were expanded to larger containers and total genomic DNA was isolated using a Qiagen DNeasy Blood and Tissue Kit (Hilden, Germany). Two PCR reactions were then performed for each clone using Standard Taq Polymerase (New England Biolabs, Ipswich, MA) to determine if deletion events took place. One PCR used primers that base paired with sequences outside of the sgRNA cut sites and should generate a truncated amplicon in exon deleted clones and (F1-CGGGAGACACTTAGAGATGTTAAA; R1-AGGAGAAAT AGCAAACGGGATA). The other PCR used primers that base paired with sequences in the region between both sgRNAs, which should be deleted in edited clones (F2-GACCCATAAGGGAAGCCTAAC; R2-ATGCCTGGT GCCACTTTAT).

2.7. Western blot

Cells were placed on ice for 10 min, washed 3X with ice cold phosphate buffered saline (PBS), and lysed with 30 μL lysis buffer (50 mM Tris pH 7.4, 150 mM NaCl, 1% Triton X-100, and protease inhibitors leupeptin (10 mg/mL), aprotinin (10 mg/mL), pepstatin (10 mg/mL), pheynyl-methylsulfonyl fluoride (1 mM)). Lysates were collected into prechilled tubes, sonicated 5 pulses each, and centrifuged at maximum speed for 10 min at 4°C in a microcentrifuge. Protein concentrations were determined using a Bradford protein assay (Hercules, CA). 100 μg of each lysate was mixed with 2X loading dye (4% (w/v) SDS, 20% (v/v) glycerol, 3.25% (v/v) 2 M Tris pH 6.8, 120 μM bromophenol blue, 100 mM dithiothreitol) and incubated at 65°C for 10 min before being subjected to SDS PAGE in 10% polyacrylamide gels. Gels were transferred to PVDF membranes (*Trans*-Blot® Turbo™ Transfer System, Bio-Rad, Hercules, CA). In order to confirm equal loading and transfer efficiency, blots were stained with ponceau stain (0.1% (w/v) Ponceau S in 5% (v/v) acetic acid). Blots were destained with 0.1 N NaOH and washed thoroughly in ddH_2O. Blots were blocked in 5% BSA in Tris Buffered Saline with 0.1% Tween-20 (TBST). Anti-CAR^{Ex8} antibody was generated against the C-terminus of CAR^{Ex8} by GenScript (Nanjing, China) with the 14AA peptide CAR^{Ex8} (CFKYPYKTDGITVV) was synthesized with an HPLC purity of > 85%. Peptide was conjugated to KLH via MBS method through the –SH of the N-terminal Cysteine residue. The peptide-KLH conjugate was used for rabbit immunization. After pre-immune screening with the peptide, two rabbits were subcutaneously immunized with 200 μg of the complex emulsified in Freund's complete adjuvant (CFA). Two boosts with 200μg each of the complex emulsified in Freund's incomplete adjuvant (IFA) were given subcutaneously after 2 and 5 weeks. After test bleed (one week after the 3rd immunization), the two animals were sacrificed for collection of the final antisera.The anti-CAR^{Ex8} antibody was purified from the antisera by peptide affinity column. Anti-CAR^{Ex8} was used at a concentration of 1:3000. Anti-total CAR (1605) antibody was generated as previously described and used at a concentration of 1:1000 (Excoffon et al., 2010; Sharma et al., 2012a). As CAR is a differentially glycosylated protein, staining can result in multiple bands (Excoffon et al., 2007). All images were taken with an Amersham Imager 600 (General Electric, Boston, MA). Bands were quantified using ImageJ analysis.

2.8. Epithelial polarization

MDCK cell lines were either semi-polarized by being grown into confluent monolayers on plastic or fully polarized by seeding on transwell inserts with 0.4 μm pores (Corning, Corning, NY) and grown at an air-liquid interface. For transwells, media was removed from the apical surface and fresh media was added to the basolateral surface every 3 days during polarization. Epithelia were considered fully polarized when the apical surface had no visible liquid and the TER measurement was above 600 Ω•cm^2 (Excoffon et al., 2010) as measured using a Volt/Ohm Meter with STX2 "chopstick" electrode (World Precision Instruments, Sarasota, FL) as previously described (Sharma et al., 2012b). The addition of doxycycline at the concentrations used in these experiments (50 and 200 ng/mL) do not prevent epithelial polarization by day 9 post seeding (Supplemental Fig. 1).

2.9. Adenovirus

Recombinant human adenovirus type 5 containing a β-galactosidase reporter gene (AdV5-LacZ) purchased from the University of Iowa Viral Vector Core with a titer of 2×10^{10} pfu/ml was used in all experiments. All infections were performed in serum free media for 1 h at 37°C at a multiplicity of infection (MOI) of ~125. After 1 h of incubation, virus was removed and cells were washed with serum free media before being placed back in complete growth media. Approximately 24 h later AdV5-LacZ transduction or viral genomes were measured as outlined below.

2.10. Quantitation of AdV5 entry and transduction

AdV5-LacZ transduction was analyzed by measuring β-galactosidase expression using the Galacto-Light Plus system from ThermoFisher Scientific (Waltham, MA) in conjunction with a Synergy H1 Microplate Reader (Winooski, VA) as previously described (Excoffon et al., 2010). Background luminescence/mg protein obtained from cells that were not infected with AdV-LacZ is subtracted off of the reported values. Viral genomes were measured via quantitative PCR (qPCR) after DNA isolation (DNeasy Blood and Tissue Kit, Qiagen, Hilden, Germany) using SYBR Green with low ROX (Quanta, Gaithersburg, MD) in a QuantStudio 7 Flex Real Time PCR System (ThermoFisher Scientific, Waltham, MA) using primers specific to the AdV5 hexon gene (F-ACGCCT CGGAGTACCTGAG and R-GTGGGGTTTCTGAACTTGT) and MDCK actin (F- AAGATCTGGCACCACACCTTCTAC and R- ATCTGGGTCATCT TCTCACGGTTG). Fold-change between samples was calculated using the $2^{-\Delta\Delta ct}$ method as previously described (Kotha et al., 2015).

3. Results

We previously created a model MDCK cell line, based on Type II MDCK cells, that stably expresses the cDNA for FLAG-tagged human CAR^{Ex8} under a doxycycline-inducible promoter (MDCK-CAR^{Ex8}) (Kotha et al., 2015). The FLAG tag resides at the extracellular N-terminus of the CAR^{Ex8} construct, but does not affect adenoviral binding or transduction (van't Hof and Crystal, 2001; Walters et al., 2001). MDCK cells offer several advantages as a model system to study epithelial biology and AdV infection. They have a relatively fast rate of cellular division, can be cloned from single cells, and have the ability polarize rapidly into monolayers with tight junctions on plastic, glass, and when grown on inserts with semi-permeable membranes such as transwells, and have been well studied in terms of epithelial morphology and physiology as well as protein expression (Dukes et al., 2011; Price et al., 2018; Rangel et al., 2019; Sharma et al., 2017). Furthermore, they recapitulate many processes, such as differential CAR isoform expression and localization, that primary human airway epithelial cells exhibit (Excoffon et al., 2010; Kotha et al., 2015; Sharma et al., 2017). While much has been learned about the function of the CAR^{Ex8} isoform in polarized epithelia by using this model cell line, data must be interpreted with the understanding that there is endogenous expression of canine CAR^{Ex8}. To further understand the functional importance of the apical CAR isoform, CRISPR/Cas9 technology was used to target genomic CAR^{Ex8} expression, while leaving the doxycycline inducible insert intact. This was done by specifically targeting the intronic regions flanking the eighth exon of the MDCK *CXADR* gene. Using this strategy leaves the genetic information necessary to encode CAR^{Ex7} intact while deleting approximately 1.3kb of the genome that contains the eighth exon of *CXADR*.

3.1. Generation and transfection of sgRNA constructs

In order to ensure the sgRNA targets would base pair properly in our cells, the region around the eighth exon of the MDCK *CXADR* gene was sequenced by Genewiz (South Plainfield, NJ). The resulting sequence was used to generate a list of potential sgRNAs using CHOPCHOP software (Labun et al., 2016; Montague et al., 2014). The criteria for selection included proximity to the eighth exon as well as the quality score provided by the program that is based on predicted cutting efficiency and potential for off target cutting elsewhere in the genome. Ultimately, we selected two sgRNA sequences, one upstream and one downstream of *CXADR* exon 8, that had at least 3 differing nucleotides with every other possible sgRNA in the genome. These sgRNA sequences were each cloned into the pspCas9(BB)-2A-GFP plasmid backbone. Both plasmids were double transfected into MDCK-CAR^{Ex8} cells in order to obtain cuts upstream and downstream of *CXADR* exon 8 to potentially allow exonic deletion.

3.2. Clone generation and screening

Two days post transfection, the pool of double transfected cells was isolated and subjected to FACS. Single GFP-positive cells were sorted into single wells of a 96-well plate and clonal populations were expanded and subjected to further analysis. Thirteen clones survived and were expanded from one round of transfection and FACS. Genomic DNA was isolated from each clone and subjected to PCR analysis with primers that recognize intronic sequence inside or outside the region expected to be deleted (Fig. 1A). To screen for exonic knockout, primers outside of the expected cut sites were used. Whereas the parental

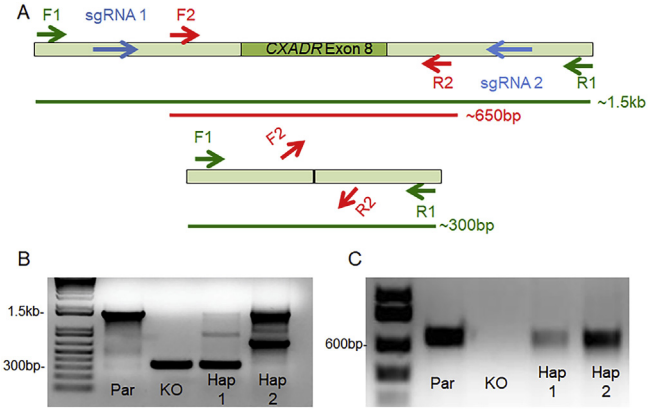

Fig. 1. *CXADR* exon 8 knockout screening. (A) Schematic of primers used to screen for deletion of the eighth exon of *CXADR* upon sgRNA cleavage upstream (sgRNA1) and downstream (sgRNA2). Expected fragment lengths for parental (above) and exon knockout (below) are shown. (B) PCR results with primers outside the cut sites comparing the untreated parental MDCK-CAR^{Ex8} cells (Par) to the knockout clone (KO; JR1-CAR^{Ex8}-KO) and two potential haploid knockout clones (Hap1 and Hap2). (C) PCR results with primers inside the cut sites comparing the untreated parental MDCK-CAR^{Ex8} cells (Par) to the knockout clone (KO; JR1-CAR^{Ex8}-KO) and two potential haploid clones (Hap1 and Hap2).

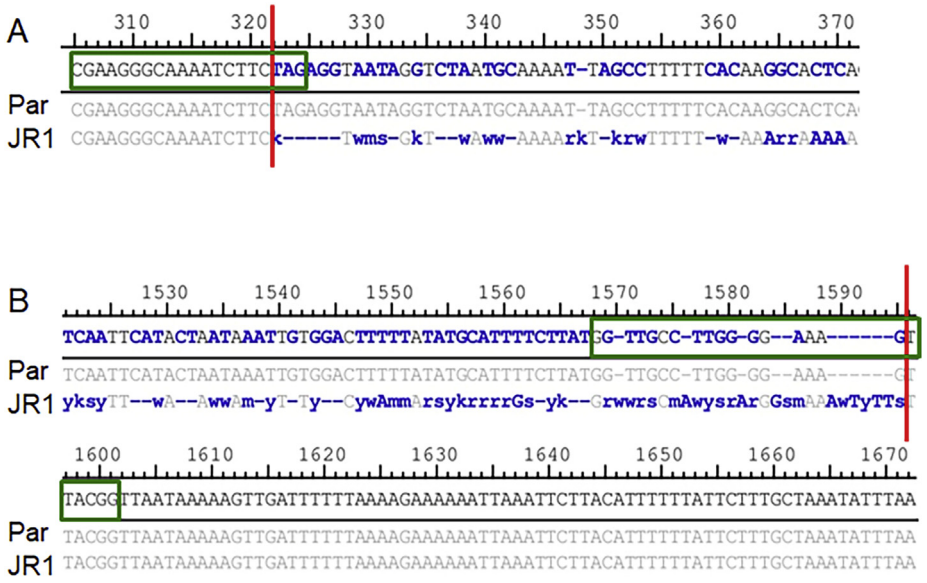

Fig. 2. Sanger sequencing of the *CXADR* exon 8 region. Comparison of the parental (Par) and JR1-CAR^{Ex8}-KO (JR1) genomic sequencing around the sgRNA (green boxes) (A) upstream or (B) downstream of the 8th exon of MDCK *CXADR*. The red line indicates the predicted cut sites for the CRISPR/Cas9-gRNA complex. The blue letters in the JR1 sequence represent the presence of indels that occurred due to Cas9 editing. The blue letters in the top sequence represent nucleotide sequences that are distinct between parental and JR1-CAR^{Ex8}-KO cells.

MDCK-CAR^{Ex8} cells produced a band at the expected size of ~1.5 kb, only 1 clone had a single truncated band at ~300bp suggesting that a deletion event had occurred in this clone (Fig. 1B). The other clones that were subjected to this PCR demonstrated multiple bands at various sizes, arguing that cutting events took place in at least one allele (Fig. 1B). As expected, primers recognizing sequence within the site expected to be deleted produced a band at ~650 bp for the parental MDCK-CAR^{Ex8} cells. The single successful clone did not produce any band (Fig. 1C). The other clones that were subjected to this PCR produced a single band at ~650 bp similar to the parental MDCK-CAR^{Ex8} cells (Fig. 1C). These results suggested that 1/13 clones had undergone the desired cutting reactions and this clone was renamed JR1-CAR^{Ex8}-KO and subjected to further analysis. Sanger sequencing revealed the presence of indels present at the expected cut sites in JR1-CAR^{Ex8}-KO cells (Fig. 2).

3.3. JR1-CAR^{Ex8}-KO cells exhibit reduced CAR^{Ex8} expression

JR1-CAR^{Ex8}-KO and MDCK-CAR^{Ex8} cells exhibited similar morphology and growth characteristics (data not shown). SDS-PAGE and Western blot analysis with an antibody that can detect both transmembrane isoforms of CAR demonstrated that total CAR protein levels (the majority of which is CAR^{Ex7}) decreased by 38% with a standard deviation of 12% (Fig. 3A). However, Western blot analysis with an antibody specific to the CAR^{Ex8} isoform demonstrated a pronounced reduction of CAR^{Ex8} by approximately 67% reduction with a standard deviation of 20% relative to parental MDCK CAR^{Ex8} cells (Fig. 3B). By contrast, overnight treatment with 200 ng/mL doxycycline induced very high and similar protein expression of total CAR and CAR^{Ex8} in both cell lines demonstrating that the lentiviral insert was not affected by CRISPR editing (Fig. 3A and B).

3.4. JR1-CAR^{Ex8}-KO exhibit reduced AdV-LacZ entry

Analysis of AdV5 infection was assessed in both partially polarized cultures on plastic and completely polarized cultures on transwells. When seeded on plastic and grown into a confluent monolayer, JR1-CAR^{Ex8}-KO cells exhibited 2X less AdV5-LacZ transduction, as measured by β-galactosidase activity per mg protein, than parental MDCK-CAR^{Ex8} cells (Fig. 4A). Furthermore, the addition of doxycycline enhanced AdV5-LacZ transduction in both cell lines, providing further evidence that the lentiviral insert is functional in the JR1-CAR^{Ex8}-KO and MDCK CAR^{Ex8} parental cell lines (Fig. 4A; the average measurements and

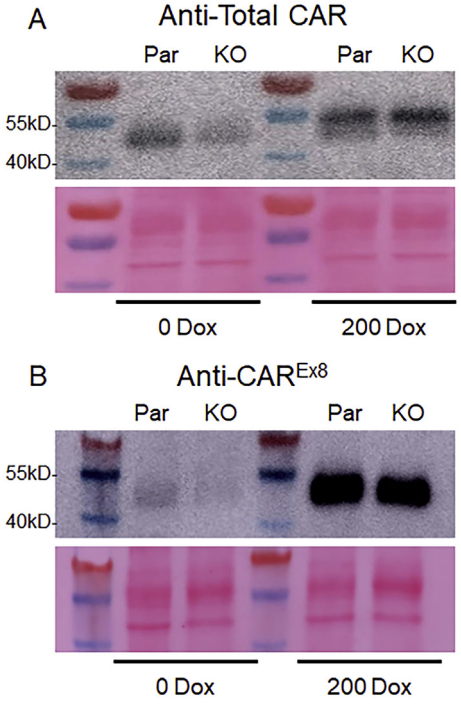

Fig. 3. Total CAR expression is partially reduced while CAR^{Ex8} expression is largely attenuated in JR1-CAR^{Ex8}-KO cells compared to MDCK-CAR^{Ex8} parental cells. MDCK-CAR^{Ex8} parental cells (Par) or JR1-CAR^{Ex8}-KO cells (KO) were exposed to either 0 or 200 ng/mL doxycycline overnight, lysed and subjected to SDS-PAGE. The blot was stained with ponceau to ensure equal loading (lower blot). Western blot with a polyclonal antibody which detects (A) both transmembrane isoforms of CAR (Rabbit-Anti-CAR-1605p) or (B) a polyclonal antibody which detects CAR^{Ex8} (Rabbit-Anti-CAR^{Ex8}). Western Blots are representative images from 3 independent experiments.

standard deviations of each condition (in Luminescence per mg protein) were 20.2 ± 8.3 x 10^5 for parental cells without doxycycline, 48 ± 1.2 x 10^5 for parental cells with doxycycline, 9.7 ± 1.6 x 10^5 for JR1-CAR^{Ex8}-KO cells without doxycycline, and 52.3 ± 8.8 x 10^5 for JR1-CAR^{Ex8}-KO cells with doxycycline). To determine differences specifically in apical AdV5-LacZ entry, both JR1-CAR^{Ex8}-KO and MDCK-CAR^{Ex8} parental cells were seeded on semi-permeable transwell membranes and grown at the air-liquid interface to allow complete epithelial

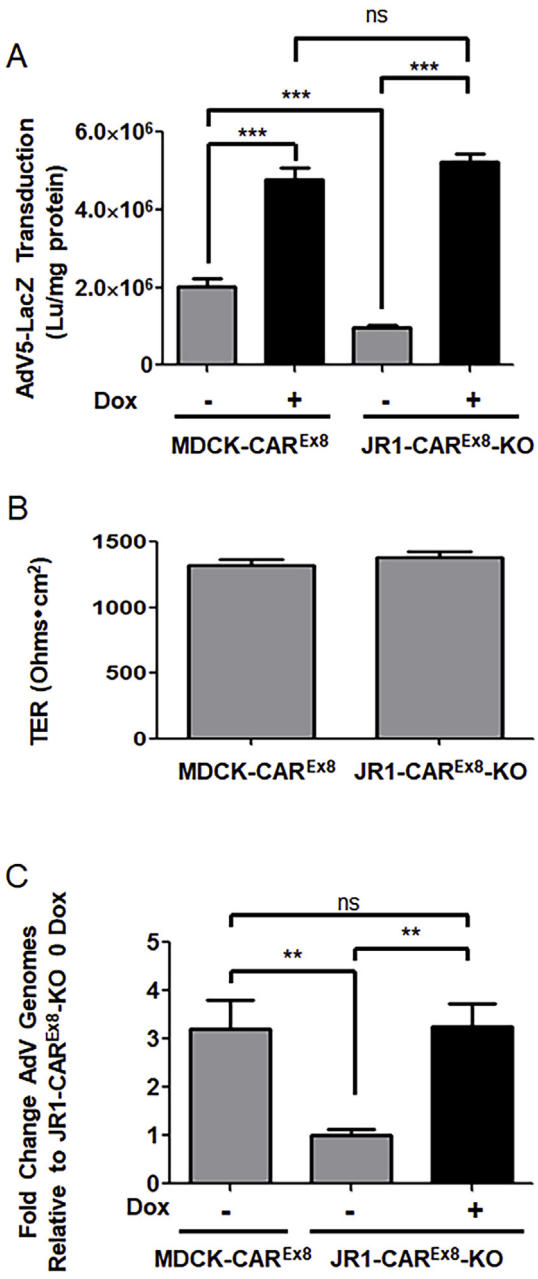

Fig. 4. Adenovirus entry is significantly attenuated in JR1-CAR^{Ex8}-KO cells compared to MDCK-CAR^{Ex8} parental cells. (A) Cells seeded on plastic and grown into confluent monolayers were treated with 0 (gray) or 50 ng/mL (black) doxycycline for ~24 h before AdV-LacZ infection. Data are compiled from 3 independent experiments each with 4 biological replicates per condition (Luminescence per mg protein). One way ANOVA followed by Bonferoni post hoc test was used to determine significance. *** $p < 0.0001$. (B) TER values obtained 9 days post seeding on transwell inserts. N = 24 biological replicates per condition. (C) Cells were polarized on transwell inserts for 9 days before exposure to 0 or 200 ng/mL doxycycline 24 h followed by apical inoculation with AdV-LacZ (MOI~125). Total DNA was isolated ~24 h later for qPCR for adenoviral genomes. Values are reported as fold change ($2^{-\Delta\Delta ct}$) from JR1-CAR^{Ex8}-KO cells in the absence of doxycycline relative to canine actin. Data are compiled from 3 independent experiments each with 4 biological replicates amplified in duplicate per condition. One way ANOVA followed by Bonferoni post hoc test was used to determine significance. ** $p < 0.001$. Error bars represent standard error of the mean.

polarization. When grown at the air-liquid interface on semi-permeable membranes, both polarized to a similar degree and achieved TER values > 1200 ohms cm^2 9 days post seeding indicating the formation of tight junctions (Fig. 4B). After apical AdV5-LacZ inoculation, the apical surface was washed to remove unbound virus. Total DNA was isolated from the cells and cell-associated viral DNA, a marker for viral entry, was measured by qPCR using AdV specific primers 24 h after inoculation. In the absence of doxycycline, JR1-CAR^{Ex8}-KO cells exhibited a 3X reduction in cell associated viral genomes relative to parental cells (Fig. 4C). Pretreatment with 200 ng/mL doxycycline restored viral genome entry in JR1-CAR^{Ex8}-KO cells to similar levels observed in parental MDCK-CAR^{Ex8} cells (Fig. 4C; Ct values with standard deviations for AdV Hexon primers were 30.9 ± 1.2 for parental, 32.2 ± 1.1 for JR1-CAR^{Ex8}-KO without doxycycline, and 30.5 ± 0.9 for JR1-CAR^{Ex8}-KO with doxycycline; control no virus (background) Ct values were 35.8 ± 1.9. Actin Ct values with standard deviation were 19.1 ± 0.4 for parental cells, 18.8 ± 0.3 for JR1-CAR^{Ex8}-KO cells without doxycycline, 18.7 ± 0.3 for JR1-CAR^{Ex8}-KO cells with doxycycline and 18.9 ± 0.3 for control no virus cells).

4. Discussion

CRISPR/Cas9 gene editing has made it possible to achieve exon-specific deletion and therefore isoform specific knockout of proteins (Bauer et al., 2015; Canver et al., 2014; Hsu et al., 2014). We adopted a gene editing procedure that relied on double transfection of plasmids that encode Cas9, sgRNAs that flank the 8th exon of the MDCK *CXADR* gene, and GFP. Following transfection, FACS sorting the cells that exhibited the highest degree of GFP positivity into single wells of a 96 well plate allowed for the enrichment of cells that were more likely to have undergone gene editing and allowed for the establishment of clonal populations. Clones were then screened for exonic deletion using PCR. Using this procedure, a polarizable epithelial cell line was obtained that exhibits reduced protein expression of CAR^{Ex8}. Expression of total CAR appears to be less affected. This discrepancy between total CAR and CAR^{Ex8} specific staining is expected to be largely due to the CAR^{Ex7} isoform. These data suggest that endogenous CAR^{Ex8} expression is significantly attenuated while CAR^{Ex7} expression is largely maintained. This makes sense, as CAR^{Ex8} has been previously reported to make up a small percentage of total CAR expression in epithelial cells (Excoffon et al., 2010; Sharma et al., 2017). Furthermore, with the addition of doxycycline, CAR^{Ex8} expression was greatly enhanced in JR1-CAR^{Ex8}-KO, indicating that the lentiviral insert is unaffected.

Our PCR results show no amplification of exon 8 in JR1-CAR^{Ex8}-KO cells when using primers that recognize the sequence that should be deleted and only a single truncated amplicon when using primers that are outside of the expected cut sites. Given this PCR profile, we were surprised to find that this cell line still had some CAR^{Ex8} detectable by Western blot. There are several possible reasons for this. Although unlikely, it is possible that one allele could still be intact, but has undergone indel formation so extensively that the primer recognition sites have been mutated. Alternatively, MDCK cells are known to be hyperdiploid and it is possible that there is another allele that could not be detected or targeted with this approach (Cassio, 2013). While genomic sequencing of the parental MDCK-CAR^{Ex8} cells was successful, sequencing of JR1-CAR^{Ex8}-KO resulted in truncated sequences that revealed extensive indel formation at the expected cut sites, but did not amplify the region between the cut sites. Although this has not been observed in other experiments, another possibility is that the CAR^{Ex8} antibody was demonstrating non-specific binding. Finally, it is possibly a leaky doxycycline-inducible lentiviral insert, however, no FLAG-tag expression is visible via Western blot, even at high loading and long exposure, in the absence of doxycycline (Supplemental Fig. 2). While future experiments are aimed at addressing the discrepancy we see between PCR results and protein expression, it is clear that there is a significant knockdown of CAR^{Ex8} protein expression which allowed us to successfully test our hypothesis about the importance of CAR^{Ex8} expression for apical AdV5 entry and transduction, particularly in a polarized epithelium.

There is approximately 25 kb of DNA between the 7th and 8th exons of *CXADR* (Fechner et al., 1999). The data presented here indicate that this distance can provide a buffer for editing and deleting only the 8th exon, while leaving the 7th exon, and therefore expression of CAR^{Ex7}, intact. The JR1-CAR^{Ex8}-KO, cell line provides a model system in which genomic CAR^{Ex8} expression is significantly attenuated, but CAR^{Ex7} expression is largely intact and CAR^{Ex8} expression can be rescued by a lentiviral insert that expresses CAR^{Ex8} with the addition of doxycycline. Using this cell line, compared to parental cells, we found a ~2X reduction in AdV5-LacZ transduction when cells were seeded on plastic and a ~3X reduction in AdV5-LacZ genome copies when cells were polarized on transwell inserts and grown at an air-liquid interface. This argues that seeding on plastic results in only partial epithelial polarization, and that specific attenuation of the CAR^{Ex8} isoform does not play as large a role in AdV5 transduction when access to basolateral CAR^{Ex7} is still available. However, when epithelial cells are fully polarized, apical infection in these epithelia relies more on CAR^{Ex8} expression. This is further corroborated by the addition of doxycycline, and therefore CAR^{Ex8} expression, which fully recovered AdV5 viral genome levels to those seen in parental cells.

The JR1-CAR^{Ex8}-KO, cell line provides a new model system to study the effects of knockdown and upregulation of CAR^{Ex8} expression on epithelial virus infection. Furthermore, future studies are likely to reveal new isoform specific cellular functions for CAR^{Ex8} such as in epithelial interactions with cells of the innate immune system and responses to inflammation. Our methods also establish an experimental pipeline to produce additional genomic CAR^{Ex8} knockdown or knockout MDCK cell lines.

Taken together, our data argue that CAR^{Ex8} is the primary receptor for apical AdV5 infection of polarized epithelia. Future studies will explore the relative effects of AdV co-receptors, methods to manipulate epithelial AdV infection that rely on, and are independent of, CAR^{Ex8} expression, and test regulation of CAR^{Ex8} expression as a potential clinical mechanism for inhibiting human AdV infections.

Acknowledgements

Research reported in this publication was supported by the National Institute of Allergy and Infectious Diseases of the National Institutes of Health under Award Numbers R15AI090625 and R01AI127816. The content is solely the responsibility of the authors and does not necessarily represent the official views of the National Institutes of Health.

Appendix A. Supplementary data

Supplementary data to this article can be found online at https://doi.org/10.1016/j.virol.2019.07.018.

References

Bauer, D.E., Canver, M.C., Orkin, S.H., 2015. Generation of genomic deletions in mammalian cell lines via CRISPR/Cas9. J. Vis. Exp. 95, e52118. https://doi.org/10.3791/52118.

Bergelson, J.M., Cunningham, J.A., Droguett, G., Kurt-Jones, E.A., Krithivas, A., Hong, J.S., Horwitz, M.S., Crowell, R.L., Finberg, R.W., 1997. Isolation of a common receptor for Coxsackie B viruses and adenoviruses 2 and 5. Science 275 (5304), 1320–1323.

Berk, A.J., 2007. *Adenoviridae*: the viruses and their replication. In: 5 ed. In: Knipe, D.M., Howley, P.M. (Eds.), Fields Virology, vol. 2. Philadelphia Lippincott Williams & Wilkins, pp. 2355–2394.

Bewley, M.C., Springer, K., Zhang, Y.B., Freimuth, P., Flanagan, J.M., 1999. Structural analysis of the mechanism of adenovirus binding to its human cellular receptor, CAR. Science 286 (5444), 1579–1583.

Canver, M.C., Bauer, D.E., Dass, A., Yien, Y.Y., Chung, J., Masuda, T., Maeda, T., Paw, B.H., Orkin, S.H., 2014. Characterization of genomic deletion efficiency mediated by clustered regularly interspaced short palindromic repeats (CRISPR)/Cas9 nuclease system in mammalian cells. J. Biol. Chem. 289 (31), 21312–21324. https://doi.org/10.1074/jbc.M114.564625.

Cassio, D., 2013. Long term culture of MDCK strains alters chromosome content. BMC Res. Notes 6, 162. https://doi.org/10.1186/1756-0500-6-162.

Chen, J.W., Zhou, B., Yu, Q.C., Shin, S.J., Jiao, K., Schneider, M.D., Baldwin, H.S., Bergelson, J.M., 2006. Cardiomyocyte-specific deletion of the coxsackievirus and adenovirus receptor results in hyperplasia of the embryonic left ventricle and abnormalities of sinuatrial valves. Circ. Res. 98 (7), 923–930. https://doi.org/10.1161/01.RES.0000218041.41932.e3.

Dukes, J.D., Whitley, P., Chalmers, A.D., 2011. The MDCK variety pack: choosing the right strain. BMC Cell Biol. 12, 43. https://doi.org/10.1186/1471-2121-12-43.

Echavarria, M., 2008. Adenoviruses in immunocompromised hosts. Clin. Microbiol. Rev. 21 (4), 704–715. https://doi.org/10.1128/CMR.00052-07.

Excoffon, K.J., Bowers, J.R., Sharma, P., 2014. 1. Alternative splicing of viral receptors: a review of the diverse morphologies and physiologies of adenoviral receptors. Recent Res Dev Virol 9, 1–24.

Excoffon, K.J., Gansemer, N., Traver, G., Zabner, J., 2007. Functional effects of coxsackievirus and adenovirus receptor glycosylation on homophilic adhesion and adenoviral infection. J. Virol. 81 (11), 5573–5578. https://doi.org/10.1128/JVI.02562-06.

Excoffon, K.J., Gansemer, N.D., Mobily, M.E., Karp, P.H., Parekh, K.R., Zabner, J., 2010. Isoform-specific regulation and localization of the coxsackie and adenovirus receptor in human airway epithelia. PLoS One 5 (3), e9909. https://doi.org/10.1371/journal.pone.0009909.

Excoffon, K.J., Traver, G.L., Zabner, J., 2005. The role of the extracellular domain in the biology of the coxsackievirus and adenovirus receptor. Am. J. Respir. Cell Mol. Biol. 32 (6), 498–503. https://doi.org/10.1165/rcmb.2005-0031OC.

Fechner, H., Haack, A., Wang, H., Wang, X., Eizema, K., Pauschinger, M., Schoemaker, R., Veghel, R., Houtsmuller, A., Schultheiss, H.P., Lamers, J., Poller, W., 1999. Expression of coxsackie adenovirus receptor and alphav-integrin does not correlate with adenovector targeting in vivo indicating anatomical vector barriers. Gene Ther. 6 (9), 1520–1535. https://doi.org/10.1038/sj.gt.3301030.

Florescu, D.F., Hoffman, J.A., AST Infectious Diseases Community of Practice, 2013. Adenovirus in solid organ transplantation. Am. J. Transplant. 13 (Suppl. 4), 206–211. https://doi.org/10.1111/ajt.12112.

Hsu, P.D., Lander, E.S., Zhang, F., 2014. Development and applications of CRISPR-Cas9 for genome engineering. Cell 157 (6), 1262–1278. https://doi.org/10.1016/j.cell.2014.05.010.

Humar, A., Kumar, D., Mazzulli, T., Razonable, R.R., Moussa, G., Paya, C.V., Covington, E., Alecock, E., Pescovitz, M.D., Group, P.V.S., 2005. A surveillance study of adenovirus infection in adult solid organ transplant recipients. Am. J. Transplant. 5 (10), 2555–2559. https://doi.org/10.1111/j.1600-6143.2005.01033.x.

Ison, M.G., 2006. Adenovirus infections in transplant recipients. Clin. Infect. Dis. 43 (3), 331–339. https://doi.org/10.1086/505498.

Khanal, S., Ghimire, P., Dhamoon, A.S., 2018. The repertoire of adenovirus in human disease: the innocuous to the deadly. Biomedicines 6 (1). https://doi.org/10.3390/biomedicines6010030.

Kolawole, A.O., Sharma, P., Yan, R., Lewis, K.J., Xu, Z., Hostetler, H.A., Ashbourne Excoffon, K.J., 2012. The PDZ1 and PDZ3 domains of MAGI-1 regulate the eight-exon isoform of the coxsackievirus and adenovirus receptor. J. Virol. 86 (17), 9244–9254. https://doi.org/10.1128/JVI.01138-12.

Kotha, P.L., Sharma, P., Kolawole, A.O., Yan, R., Alghamri, M.S., Brockman, T.L., Gomez-Cambronero, J., Excoffon, K.J., 2015. Adenovirus entry from the apical surface of polarized epithelia is facilitated by the host innate immune response. PLoS Pathog. 11 (3), e1004696. https://doi.org/10.1371/journal.ppat.1004696.

Labun, K., Montague, T.G., Gagnon, J.A., Thyme, S.B., Valen, E., 2016. CHOPCHOP v2: a web tool for the next generation of CRISPR genome engineering. Nucleic Acids Res. 44 (W1), W272–W276. https://doi.org/10.1093/nar/gkw398.

Lion, T., 2014. Adenovirus infections in immunocompetent and immunocompromised patients. Clin. Microbiol. Rev. 27 (3), 441–462. https://doi.org/10.1128/CMR.00116-13.

Montague, T.G., Cruz, J.M., Gagnon, J.A., Church, G.M., Valen, E., 2014. CHOPCHOP: a CRISPR/Cas9 and TALEN web tool for genome editing. Nucleic Acids Res. 42, W401–W407. https://doi.org/10.1093/nar/gku410. (Web Server issue).

Price, A.J., Cost, A.L., Ungewiss, H., Waschke, J., Dunn, A.R., Grashoff, C., 2018. Mechanical loading of desmosomes depends on the magnitude and orientation of external stress. Nat. Commun. 9 (1), 5284. https://doi.org/10.1038/s41467-018-07523-0.

Ran, F.A., Hsu, P.D., Wright, J., Agarwala, V., Scott, D.A., Zhang, F., 2013. Genome engineering using the CRISPR-Cas9 system. Nat. Protoc. 8 (11), 2281–2308. https://doi.org/10.1038/nprot.2013.143.

Rangel, L., Bernabe-Rubio, M., Fernandez-Barrera, J., Casares-Arias, J., Millan, J., Alonso, M.A., Correas, I., 2019. Caveolin-1 alpha regulates primary cilium length by controlling RhoA GTPase activity. Sci. Rep. 9 (1), 1116. https://doi.org/10.1038/s41598-018-38020-5.

Sharma, P., Kolawole, A.O., Core, S.B., Kajon, A.E., Excoffon, K.J., 2012a. Sidestream smoke exposure increases the susceptibility of airway epithelia to adenoviral infection. PLoS One 7 (11), e49930. https://doi.org/10.1371/journal.pone.0049930.

Sharma, P., Kolawole, A.O., Wiltshire, S.M., Frondorf, K., Excoffon, K.J., 2012b. Accessibility of the coxsackievirus and adenovirus receptor and its importance in adenovirus gene transduction efficiency. J. Gen. Virol. 93 (Pt 1), 155–158. https://doi.org/10.1099/vir.0.036269-0.

Sharma, P., Martis, P.C., Excoffon, K., 2017. Adenovirus transduction: more complicated than receptor expression. Virology 502, 144–151. https://doi.org/10.1016/j.virol.2016.12.020.

van't Hof, W., Crystal, R.G., 2001. Manipulation of the cytoplasmic and transmembrane domains alters cell surface levels of the coxsackie-adenovirus receptor and changes the efficiency of adenovirus infection. Hum. Gene Ther. 12 (1), 25–34. https://doi.org/10.1089/104303401450933.

Walters, R.W., Freimuth, P., Moninger, T.O., Ganske, I., Zabner, J., Welsh, M.J., 2002.

Adenovirus fiber disrupts CAR-mediated intercellular adhesion allowing virus escape. Cell 110 (6), 789–799.

Walters, R.W., van't Hof, W., Yi, S.M., Schroth, M.K., Zabner, J., Crystal, R.G., Welsh, M.J., 2001. Apical localization of the coxsackie-adenovirus receptor by glycosyl-phosphatidylinositol modification is sufficient for adenovirus-mediated gene transfer through the apical surface of human airway epithelia. J. Virol. 75 (16), 7703–7711. https://doi.org/10.1128/JVI.75.16.7703-7711.2001.

Yan, R., Sharma, P., Kolawole, A.O., Martin, S.C., Readler, J.M., Kotha, P.L., Hostetler, H.A., Excoffon, K.J., 2015. The PDZ3 domain of the cellular scaffolding protein MAGI-1 interacts with the Coxsackievirus and adenovirus receptor (CAR). Int. J. Biochem. Cell Biol. 61, 29–34. https://doi.org/10.1016/j.biocel.2015.01.012.

Zen, K., Liu, Y., McCall, I.C., Wu, T., Lee, W., Babbin, B.A., Nusrat, A., Parkos, C.A., 2005. Neutrophil migration across tight junctions is mediated by adhesive interactions between epithelial coxsackie and adenovirus receptor and a junctional adhesion molecule-like protein on neutrophils. Mol. Biol. Cell 16 (6), 2694–2703. https://doi.org/10.1091/mbc.e05-01-0036.